Immunity 25, 203–211, August 2006 ©2006 Elsevier Inc. DOI 10.1016/j.immuni.2006.05.015

Altered Peptide Ligands Induce Delayed CD8-T Cell Receptor Interaction—a Role for CD8 in Distinguishing Antigen Quality

Pia P. Yachi,[1] Jeanette Ampudia,[1] Tomasz Zal,[1,2] and Nicholas R.J. Gascoigne[1,*]

[1] Department of Immunology
The Scripps Research Institute
10550 North Torrey Pines Road
La Jolla, California 92037

Summary

How T cells translate T cell receptor (TCR) recognition of almost identical pMHC ligands into distinct biological responses has remained enigmatic. Although differences in affinity or off rate are important, they offer at best an incomplete explanation. By using Förster resonance energy transfer (FRET), we have visualized the ligand-induced interaction between OT-I TCR and CD8. We found that both recruitment of TCR to the immunological synapse and the TCR-CD8 interaction induced by weak agonists (positive-selecting ligands) was delayed but not necessarily weaker than strong agonists (negative selectors). A delayed and perhaps longer lasting CD8-TCR interaction results in delayed phospho-ERK recruitment to the synapse. The kinetics of the TCR-CD8 interaction can reconcile previously anomalous data, where biological activity did not correlate with TCR-pMHC binding kinetics for certain ligands. Our findings indicate that the T cell translates antigen recognition into T cell responses by differential recruitment of CD8 to the TCR.

Introduction

Activation of mature T cells and differentiation of developing thymocytes requires ligation of the T cell receptor (TCR) by peptide-MHC (pMHC) complexes. The TCR signaling machinery can somehow distinguish between pMHC ligands that differ by even a single amino acid and translates this into different effector functions (Gascoigne et al., 2001; Germain, 2001). Altered peptide ligands (APLs) are peptide variants derived from the original antigenic peptide, with substitutions at particular residue(s). APLs can be grouped into different categories: full agonists, which are capable of complete T cell activation; weak or partial agonists; antagonists (ligands that can inhibit the activity of agonist); and others that do not stimulate the T cell (nonstimulatory ligands).

The strength of interaction between TCR and pMHC is a major factor in determining the fate of developing T cells (Alam et al., 1996), but this is also influenced by many other factors including the amount of coreceptor, pMHC density, and variation in amounts of negative regulators such as CD5 (Starr et al., 2003; Werlen et al., 2003). Strong agonists are typically recognized by the TCR with relatively high affinity and/or a long half-life. At least in class I-restricted systems, strong agonists cause negative selection, whereas lower-affinity ligands, either weak agonists or antagonists, cause positive selection of TCR transgenic thymocytes in fetal thymic organ culture (FTOC) (Alam et al., 1996, 1999; Chidgey and Boyd, 1998; Hogquist et al., 1994, 1995; Holmberg et al., 2003; Jameson et al., 1994; Sebzda et al., 1996). Models for how T cells are activated by low numbers of antigenic pMHC and how they are able to distinguish between different pMHCs generally fall into those based on kinetic proofreading, where discrimination between ligands is based on kinetic parameters, primarily the half-life of TCR-pMHC binding, and those that invoke architectural or conformational changes in the signaling complex (Germain, 2001). The general correlation between biological activity and TCR-pMHC binding half-life is predicted by kinetic proofreading, but there are numerous exceptions to this correlation (Gascoigne et al., 2001). In contrast, there is little evidence from TCR structures supporting conformational change as a means to differentiate between ligands, with the exception of one crystal structure that shows conformational changes in the Cα domain of pMHC bound TCR compared to unliganded TCR, in a region predicted to interact with CD3ε (Kjer-Nielsen et al., 2003). Other data suggest that binding of an agonist or negative selecting ligand, but not of a positive-selecting ligand, exposes a normally hidden SH3 binding site in CD3ε that then binds to the signaling adaptor molecule, Nck (Gil et al., 2002; Risueno et al., 2006).

In addition to the TCR signal, the coreceptors, CD4 on T helper cells and CD8 on cytotoxic T cells (CTL), are crucial in thymocyte development and are generally required for effective T cell activation. For $CD8^+$ cells, this coreceptor modulates the strength of signaling through the TCR by delivering CD8-associated Lck to the TCR complex (Veillette et al., 1988). The coreceptors also enhance adhesion by binding to nonpolymorphic regions of pMHC (Gao et al., 1997; Norment et al., 1988). Both of these molecular associations are thought to contribute to stabilization of TCR-pMHC complex. They have a role in discrimination between different types of ligands in that interfering with the ability of coreceptor to interact with the TCR-pMHC complex converted an agonist into a partial agonist (Madrenas et al., 1997). Also, the amount of CD8 in the thymocytes determined whether a given T cell clone is positively or negatively selected (Starr et al., 2003; Werlen et al., 2003). We have previously shown that close proximity between coreceptor and TCR is induced by agonist pMHC but not by nonstimulatory or antagonist ligands (Gascoigne and Zal, 2004; Yachi et al., 2005; Zal et al., 2002). So far, there has not been a study correlating the interaction between TCR and coreceptor with TCR-pMHC binding kinetics and T cell activation by different APLs. Several APLs for the OT-I TCR have been particularly well defined in terms of their activation or antagonism of mature $CD8^+$ T cells and for their ability to induce positive and negative selection in thymic development (Hogquist et al., 1994, 1995; Jameson et al., 1994; Rosette et al., 2001). Moreover, the solution

*Correspondence: gascoigne@scripps.edu

[2] Present address: Department of Immunology, MD Anderson Cancer Center, University of Texas, Houston, Texas 77030.

binding kinetics of the OT-I TCR have been measured for these different pMHC complexes, and "outliers" were identified from the otherwise compelling correlation between the affinity and half-life of pMHC-TCR complexes and the biological outcomes (Alam et al., 1996, 1999; Gascoigne et al., 2001; Rosette et al., 2001).

Förster (or fluorescent) resonance energy transfer (FRET) microscopy allows us to quantitate the extent and kinetics of molecular interactions between fluorophore-tagged proteins within a subcellular region such as the immunological synapse (Zal and Gascoigne, 2004). FRET works only between molecules less than ~10 nm apart, making it useful to show molecular interactions in a nondestructive way. To this end, we have measured the kinetics of TCR-CD8 interaction by using FRET between CD8β-yellow fluorescent protein (YFP) and CD3ζ-cyan (C)FP, during recognition of a range of APLs in the OT-I T cell system. We found that different APLs induce quantitatively and qualitatively different CD8-TCR interaction profiles. Weaker agonists induced FRET between CD8 and TCR slower than the full agonist. The slower kinetics correlated with delays in the appearance of phosphorylated kinase ERK (pERK) at the synapse. Moreover, the kinetics and magnitude of TCR-CD8 interaction induced by different APLs, including "outlier APLs," correlated better with their biological strength than the kinetics of corresponding TCR-pMHC interaction in solution. Thus, the T cell uses different kinetics of CD8 recruitment to the TCR to translate altered antigen recognition signals into distinct functional responses.

Results

Bioactivity of APLs in the OT-I System

Chimeric CD8β-YFP (Yachi et al., 2005) and CD3ζ-CFP (Zal et al., 2002) genes were retrovirally introduced into CD8-negative OT-I hybridomas previously transfected with wild-type CD8α, giving rise to a stable cell line (OT-I.ZC.8βY). Enhanced cyan fluorescent protein (ECFP) and enhanced yellow FP (EYFP) are a well-characterized donor-acceptor pair of fluorescent proteins for FRET microscopy (Yachi et al., 2005; Zal and Gascoigne, 2004; Zal et al., 2002). The OT-I TCR recognizes an ovalbumin-derived peptide (OVA) presented by H-2K^b and a series of APLs with single amino acid substitutions. The activation (agonist or antagonist), thymocyte selection (negative or positive) phenotypes, and solution binding kinetics for these APLs are summarized in Table S1 (in the Supplemental Data available with this article online). The relationship between the biological activity of these APLs and their solution binding kinetics is good, but not complete: e.g., A2 is 10%–20% the strength of OVA, but still a strong agonist (Hogquist et al., 1995). However, K^b-A2 binds OT-I TCR with a slightly higher affinity and longer half-life than does K^b-OVA (Alam et al., 1999). G4 is a weak agonist and an antagonist that gives positive selection in FTOC. It is inefficient at inducing early responses in T cells, but gives strong responses at late time points (Rosette et al., 2001). It has very slow association and dissociation rates, i.e., its half-life is much longer than the strong agonists.

Equal Opportunity Antigen Presentation

In order to separate the effect of peptide structure from the surface density of pMHC, we used RMA-S cells as antigen-presenting cells (APC). These cells are deficient in the Tap2 peptide transporter and therefore unable to express properly folded MHC class I complexes. However, at a below-physiological temperature, they can express labile K^b or D^b molecules, which can then be stabilized by exogenously added peptide, rendering them stable when the temperature is raised to 37°C (Ljunggren et al., 1990). Different peptides have different abilities to stabilize the pMHC complexes on the cell surface; so, to ensure that the T cells are presented with equivalent numbers of pMHC complexes on the cell surface for all the APLs to be tested, we titrated the peptides and determined the loading concentration of peptide that resulted in equivalent cell-surface K^b expression, as previously described (Figure 1A; Holmberg et al., 2003; Yachi et al., 2005). The pMHC expressions remained stable for more than 60 min (data not shown).

High-Affinity Ligands Induce CD3ζ Recruitment Faster than Lower-Affinity Ligands

To relate earlier biological data on APLs to our assays, we tested the ability of the different peptides to induce TCR downregulation, T-APC conjugate formation, and the recruitment of TCR and CD8 to the synapse. TCR downregulation in the OT-I.ZC.8βY T hybrids was tested with RMA-S cells loaded to equivalent pMHC density (Figure 1B). OVA downregulated TCR with very fast kinetics: 50% downregulation was achieved in less than 20 min, and maximum (>95%) downregulation by 90 min. The strong agonist A2 downregulated TCR as strongly as OVA, with very slightly slower kinetics. The weak agonist or antagonist G4 never fully downregulated TCR, reaching a plateau of ~60% downregulation by 2 hr. The antagonist E1 showed very weak TCR downregulation, plateauing at 15% at 90 min. (E1 may also be considered a very weak agonist in that it can sensitize target cells for weak CTL-mediated killing [Hogquist et al., 1994].) The pure antagonist R4 showed no more than 6% downregulation even after 3 hr, and nonstimulatory peptide VSV gave no marked TCR downregulation. The ability of these APLs to cause endocytosis of the TCRs correlated well with the qualitatively different functional responses that they induce.

Formation of conjugates between the T cells and RMA-S cells presenting the different APLs was compared by flow cytometry. Cy5-labeled RMA-S cells were loaded with peptides and mixed with OT-I.ZC.8βY cells. T-APC conjugates were counted by comparing events positive for both YFP (OT-I.ZC.8βY) and Cy5 (RMA-S cells) to the total number of OT-I.ZC.8βY cells (Figure 1C). Most of the ligands showed a similar time course of conjugate formation, peaking at 15–20 min, with the number of conjugates being in proportion to the relative strength of the ligands in T cell activation. Note that all of the APLs and the nonstimulatory peptide VSV promoted conjugate formation compared to RMA-S cells without added peptide. We have shown previously that several different endogenous nonstimulatory peptides promote conjugate formation similarly to VSV (Yachi et al., 2005).

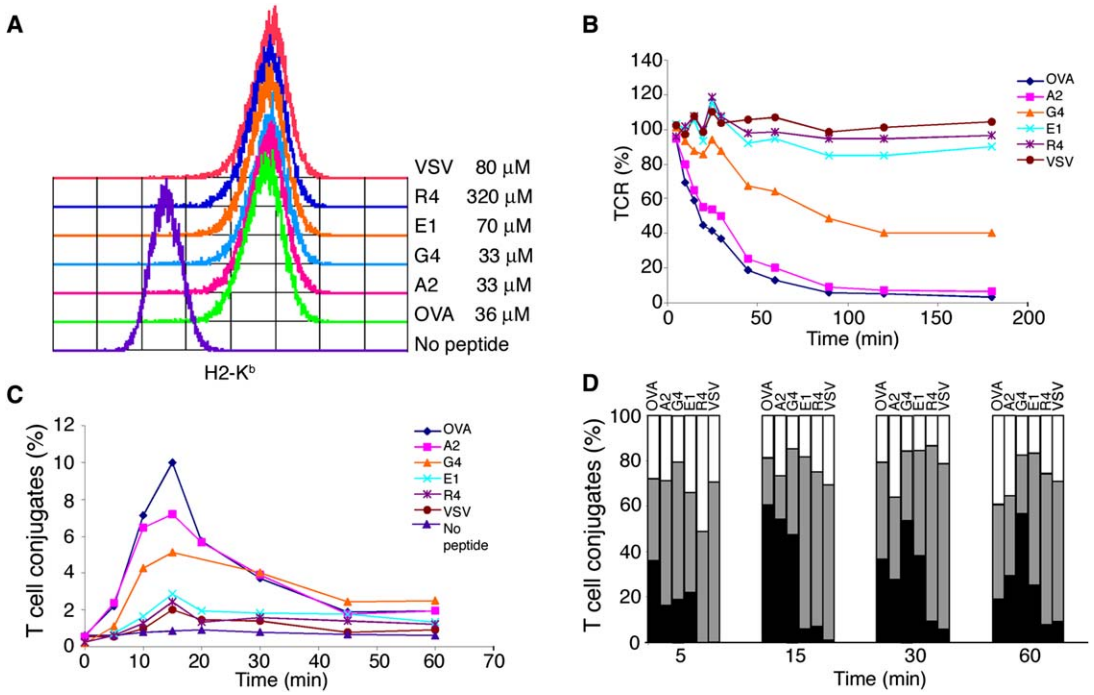

Figure 1. Effect of Different APLs on TCR Downregulation, Cell Couple Formation, and Synapse Formation

(A) In order to compare recognition of equivalent numbers of pMHC for each of the APLs, RMA-S cells were loaded with different peptides by incubating the cells at 29°C at the indicated concentrations, and subsequently at 37°C to destroy empty MHC molecules. These concentrations had been determined by titration to give equal H-2K^b density, as demonstrated by K^b Ab staining. This staining was performed with each experiment.

(B–D) OT-I.ZC.8βY cells were allowed to interact at 37°C with RMA-S cells expressing the same pMHC density of the different peptides as indicated. At various times, cells were fixed, stained, and analyzed.

(B) T cells were stained with Vβ5 Ab, and TCR expression was assessed by flow cytometry. The TCR expression is shown normalized to expression on T cells incubated with RMA-S cells in the absence of peptide (100%). Staining with an isotype control Ab was defined as 0%. The results are representative of at least three independent experiments.

(C) The time course of T-APC cell conjugate formation with different APLs was determined by flow with Cy5-labeled RMA-S cells. Cells were fixed and conjugate formation was assessed by counting the percentage of cell couples positive for both YFP and Cy5. The results are representative of at least three independent experiments.

(D) Conjugates were sorted as in (C) and imaged to determine the recruitment of CD3ζ-CFP and/or CD8β-YFP into the contact interface, in comparison to the unengaged part of the cell. The cells were grouped according to their recruitment of CD3ζ-CFP and CD8β-YFP, those with both molecules in excess in the synapse compared to the rest of the cell (black bars), those with recruitment of CD8β-YFP but not CD3ζ-CFP (gray bars), and those where neither of the molecules was at an increased level compared to the nonsynapse part of the cell (white bars). For each group, n > 29 cells (average of 46 cells). Results are representative of at least two independent experiments.

TCR-CD3ζ recruitment to the synapse requires initial stimulation through TCR. Therefore, we quantitated how the kinetics of CD3ζ-CFP recruitment correlate with APL strength. T-APC conjugates were sorted as in Figure 1C and imaged to assess the recruitment of CD3ζ-CFP and CD8β-YFP to the synapse. The cell couples were triaged into those with recruitment of both CD8 and CD3ζ, those with recruitment of CD8 alone, and those showing recruitment of neither CD8 nor CD3ζ to the synapse. We did not observe cells that recruited CD3ζ but not CD8. A much smaller proportion of cells made conjugates in response to the weak ligands such as VSV, compared to the strong ligands such as OVA, so that data on CD3ζ and CD8β recruitment for VSV could only be obtained for these relatively rare cells. The strong agonists recruited CD3ζ to the synapse area earlier than did the weaker agonists (Figure 1D). E1 gave very weak and delayed CD3ζ recruitment. The antagonist R4 and the nonstimulatory VSV recruited CD3ζ over background only in rare instances and only at later time points. Therefore, there was a good correlation between TCR recruitment to the synapse and the biological response, although G4 showed delayed kinetics, as with conjugate formation and TCR endocytosis, perhaps related to its slow on and off rates.

Delayed CD8-CD3ζ Interaction Induced by Weaker Agonists

We compared the FRET signals induced between CD3ζ-CFP and CD8β-YFP by the different agonist and antagonist APLs for the OT-I TCR. Cy5-labeled RMA-S cells were loaded with the different APLs and incubated with OT-I.ZC.8βY cells. The cells were fixed at different times and imaged, and FRET efficiency was measured in the regions of intercellular contacts (Figures 2 and 3; Yachi et al., 2005; Zal and Gascoigne, 2004). Note that these measurements are made, as for the CD8β and CD3ζ recruitment experiments described above, on individual cell-cell conjugates. Thus, for some peptides, this represents data from the low proportion of cells that actually made conjugates, compared to the relatively large proportion of cells that made conjugates in

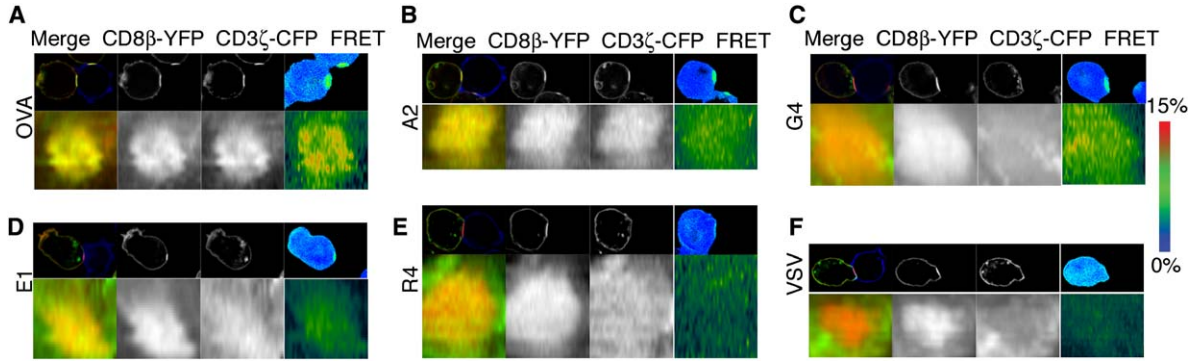

Figure 2. Recruitment of TCR and CD8, and Induction of TCR-CD8 FRET by Different APLs

OT-I hybridomas expressing CD8α wild-type, CD3ζ-CFP, and CD8β-YFP (OT-I.ZC.8βY) were incubated with Cy5-stained RMA-S cells expressing equivalent amounts of K^b loaded with the different APLs: (A) OVA, (B) A2, (C) G4, (D) E1, (E) R4, or (F) VSV. The top row of each panel shows mid-cell sections of fluorescence images (CD8β-YFP in red, CD3ζ-CFP in green, and Cy5 in blue in the merge column), and donor-ratioed, compensated FRET efficiency images in the right column. See scale bar for color coding. The bottom row of each panel shows en face projections of the T cell-APC interface and donor-ratioed compensated FRET images (right column). The contact areas between T cell and APC were defined in 3D by the overlap of Cy5 and YFP or CFP fluorescence. Original magnification: ×63. The results are representative of at least three independent experiments.

response to OVA. Such analysis emphasizes molecular events on a single-cell level while the overall outcome will be further magnified by differences in the degree of conjugate formation. As described before, the nonstimulatory peptide VSV did not increase the FRET signal in T-APC conjugates, whereas the agonist OVA induced a fast FRET response peaking 10–12 min after initiation of contact formation (Yachi et al., 2005).

The prototype OVA peptide and the APLs reported to have agonist, antagonist, and/or positive selection activity—A2, G4, E1, and R4—all, at various time points, induced in synapses a degree of FRET, hence proximity of CD3ζ-CFP to CD8β-YFP above the steady basal signal seen with VSV-loaded RMA-S cells (Figures 2 and 3). OVA induced by far the highest immediate increase in FRET at 5 min (the earliest point that could be measured) and peaked at 10 min (Figure 3A). In general, the induction of CD3ζ proximity to CD8 was lower and/or slower by APLs than by OVA. The next strongest agonist, A2, showed only slightly lower initial CD3ζ-CD8 interaction at 5 min and a delayed maximum compared to OVA. The magnitude of the interaction was lower than OVA and weaker than might have been predicted from its high-affinity binding in vitro. The weak agonist or antagonist G4 did not induce substantial FRET at 5 min but followed slowly to a strong peak of interaction at 20 min that was as strong as that induced by OVA at 10 min (Figure 3A). Antagonist E1 induced a similar time course of CD3ζ-CFP proximity to CD8β-YFP as G4, i.e., late accumulation at 20 min but with a weaker signal (Figure 3B). The pure antagonist R4 induced even lower late FRET signals, but clearly higher than VSV (Figure 3B). There were statistically significant differences between responses to all the peptides at one time point at least, except between A2 and E1 (Figure 3C). The finding that A2 did not induce a strong early TCR:CD8 interaction could explain why it is a weaker agonist than OVA, despite the slightly stronger binding of K^b-A2 to the OT-I TCR (Alam et al., 1999). Thus, the time course of TCR-CD8 FRET correlated with the phenotype of the APL in inducing positive or negative selection.

APL Independence of CD8-pMHC Interaction

At this point, we had to consider the possibility that CD8 might bind to different APL-MHC complexes with different affinities. For example, the CD8 interaction with K^b-A2 could be weaker than for K^b-OVA. However, this appeared unlikely given that the CD8 binding site on MHC is far removed from the peptide binding groove (Gao et al., 1997). To test the TCR-independent binding of CD8 to K^b peptides, we used the TCR-deficient $58\alpha^-\beta^-$ T hybridoma-expressing CD8α wild-type and CD8β-YFP ($CD8^+$) or YFP alone ($CD8^-$). These cells were mixed with Cy5-labeled RMA-S cells expressing the same amounts of K^b with the various peptides and used in a conjugate assay as above. In the absence of added peptide, the $CD8^+$ cells did not bind to the RMA-S cells (Figure 4A). The $CD8^-$ cells did not bind to the RMA-S cells with or without peptide. Thus, the cell:cell binding assay measured MHC class I and CD8-dependent binding. We found that there was no substantial difference in CD8-dependent binding to any of the K^b peptides (Figure 4A). Therefore, the differences between APLs in the induction of FRET between CD3ζ and CD8 were not trivial and had to involve TCR binding.

CD8 Dependence of A2 Stimulation

Because of the early but weaker interaction between CD8β and CD3ζ induced by A2 compared with OVA, despite its relatively "strong" phenotype as an agonist and its high-affinity TCR binding in vitro, we wondered whether recognition of A2 by OT-I TCR might somehow be independent of CD8 function. We took a short-term cultured line of ex vivo OT-I CTL and activated them with A2 or OVA in the presence of various concentrations of blocking CD8α mAb. The response to A2 was substantially more sensitive to blocking by CD8 antibody than the response to OVA. Similar results were obtained with another CD8α mAb (53-6.7, data not shown). These data indicate that OT-I activation by A2 is even more dependent than OVA on the coreceptor CD8 and that the weaker FRET response to A2 than to OVA was not due to CD8 independence of A2 recognition.

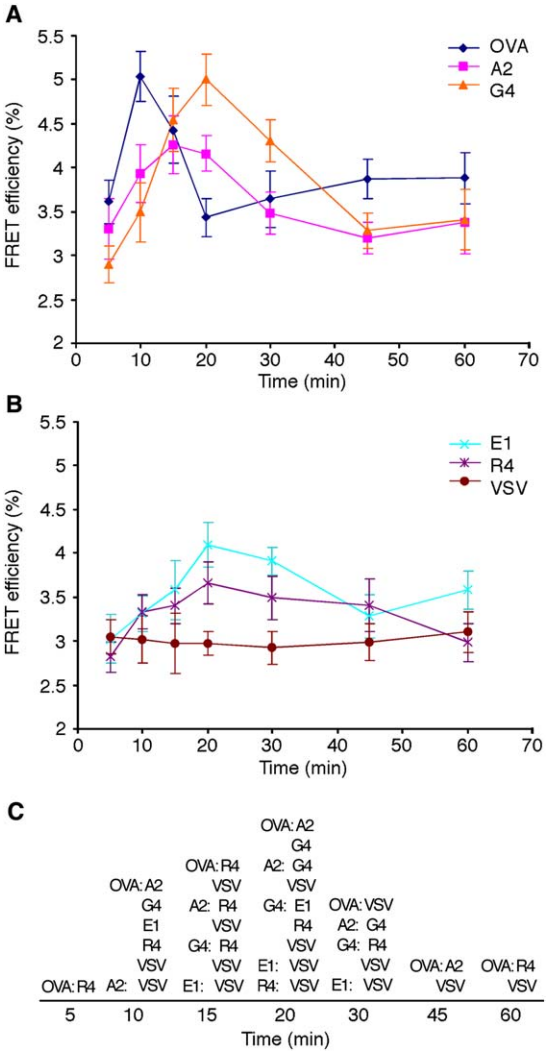

Figure 3. Delayed and Reduced Interaction between CD8 and CD3ζ with Weaker Ligands

(A and B) OT-I.ZC.8βY cells were allowed to interact with OVA, A2, G4, E1, R4, or VSV peptide-loaded RMA-S cells, and the cells were fixed at the indicated time points. FRET efficiency was assessed from the contact interface of the two cells as described for Figure 2. The results are shown as average FRET efficiency ± SEM for $n \geq 17$ (average of 29 cells, except R4 5 min, n = 11). $p < 0.05$ for OVA 10 min and G4 20 min compared to all other peptides at those time points. (C) p values < 0.05 for comparisons between different peptides are shown for each time point. The data are representative of two independent experiments.

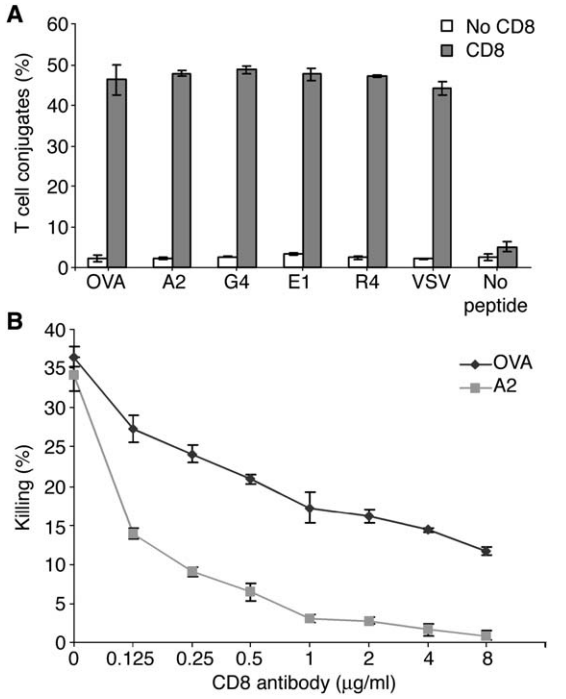

Figure 4. Comparison of APLs in Supporting K^b-CD8 Binding and CD8 Dependence of A2

(A) The different APLs were tested for their ability to support cell-cell adhesion mediated by CD8-MHC class I interaction. TCR-negative $58\alpha^-\beta^-$ hybridomas expressing CD8α wild-type and CD8β-YFP (gray bars) or $58\alpha^-\beta^-$ expressing YFP (open bars) were allowed to interact with Cy5-labeled RMA-S cells expressing the same density of different pMHC for 1 hr at 4°C. The cells were fixed and conjugates counted by flow. The results are presented as mean ± SD, n = 3, and are representative of three independent experiments.

(B) OT-I CTL were incubated ± various concentrations of inhibitory CD8α (CT-CD8α) Ab and tested at an effector:target ratio of 5:1 with ^{51}Cr-labeled EL-4 cells that had been peptide loaded with 20 nM OVA or 80 nM of A2. These amounts of peptide had been determined by titration to give an equivalent amount of CTL killing in the absence of CD8 Ab. The results are shown as mean ± SD, n = 3, and are representative of three independent experiments.

pERK Recruitment to the Synapse Correlates with CD8-CD3ζ Interaction

CD8 is thought to increase signal transduction by bringing its associated Lck molecule to the TCR complex, in order to phosphorylate the immunoreceptor tyrosine-based activation motifs (ITAM) on CD3 and ZAP-70 molecules. Phosphorylation of the MAP kinase ERK is far downstream of Lck signaling, part of the Ras signaling pathway, and has been shown to be an important corollary of signaling for positive or negative selection in thymocyte development (Werlen et al., 2003). In addition, ERK phosphorylation is an important component, with SHP-1, of positive and negative feedback loops in T cell signaling (Stefanova et al., 2003). Therefore, we wanted to compare the synapse-proximal CD8-CD3ζ interaction data with the downstream induction of pERK. OT-I.ZC.8βY cells were incubated with RMA-S cells expressing different K^b-peptide complexes for different times at 37°C. After fixing and permeabilization, the cells were stained for pERK and the signal was quantitated in the synapse (Figure 5). For OVA, the absolute amount of pERK at the synapse increased to a peak at ~20 min, then declined (Figure 5C). However, when we compared this to a plot of the ratio of pERK in the synapse compared to nonsynapse regions of the membrane of the same cells (pERK polarization to the synapse; Figure 5D), the peak was earlier. Thus, pERK was concentrated at the synapse earlier than the maximum amount of pERK was produced. The weaker agonists A2 and G4 showed lower amounts of pERK in the synapse than with OVA, and they in turn had higher amounts than the antagonists, which were barely increased relative to nonstimulatory VSV (Figure 5C). Comparison of these ligands by means of pERK polarization to the synapse as a measure (Figure 5D) showed that available pERK was

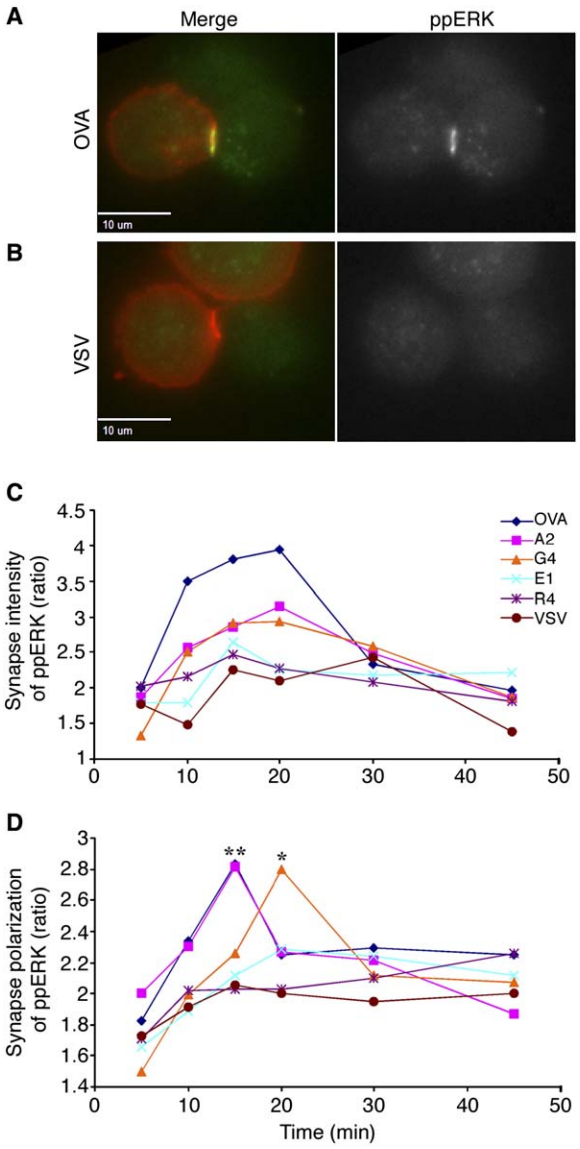

Figure 5. The Timing and Strength of ERK Phosphorylation at the Synapse Correlates with the Strength of the Induced TCR-CD8 FRET Response, rather than with Biological Activity

OT-I.ZC.8βY cells were allowed to interact with RMA-S cells expressing the same amounts of the different pMHC for various times, then fixed and stained for pERK-1 and pERK2.

(A) The localization of pERK at the synapse with RMA-S cells presenting OVA. In the merge column, CD8β-YFP is shown in red and pERK in green, and therefore yellow shows colocalization.

(B) Same as (A) except VSV peptide was used.

(C) The pERK intensity at the synapse compared to membrane of a nonstimulated cell. Background (bkg) was determined from a cell-free area of the field. For each cell, (average pixel intensity at synapse − bkg)/(average intensity at membrane of nonstimulated cell − bkg) was calculated. Determined from n > 11 cells for each peptide per time point (average of 22 cells).

(D) Polarization of pERK in the synapse compared to the nonsynapse cell surface of the same cell, from the same images as (C). For each cell (average intensity at synapse − bkg)/(average intensity of a similar-sized nonsynapse region of cell surface − bkg) was calculated. OVA and A2 are significantly different ($p < 0.05$) from all the other peptides (except from each other) at 15 min (indicated by **). G4 is significantly different from all the other peptides at 20 min (*). The experiment is representative of at least two independent experiments.

concentrated in the synapse with the same time course for the two strong agonists (negative selectors) OVA and A2, even though A2 induced a lower amount of pERK. The peak of polarization to the synapse was the same for the weak agonist (positive selector) G4, but was delayed compared to OVA or A2, as seen for the FRET response. The kinetics of the ratio for antagonist E1 were also similar to the FRET time course. Overall, these data indicate that the time course of the FRET response (TCR-CD8 interaction) is more closely related to the biological activity than is the strength of the FRET signal: i.e., strong agonists and negative selectors peak early and positive selectors peak later, although antagonists induce relatively little FRET compared to agonists. The time course of concentration of pERK in the synapse correlates with the FRET time course and bioactivity, whereas the amount of pERK that concentrates in the synapse is proportional to agonist strength. This is in accord with data showing the role of pERK and SHP-1 in defining an antagonist versus an agonist signal (Stefanova et al., 2003).

Discussion

We show here that the recruitment of TCR-CD3ζ and CD8 to the synapse and the induction of the CD3ζ and CD8 interaction contribute to the biological activity of individual APLs. There was a time delay before the induction of this interaction for some peptides, which was longer for weaker agonists. Similarly, the weaker ligands showed a delay in recruitment of pERK to the synapse compared to strong agonists. We measured molecular interaction between TCR-CD3ζ and CD8 by using FRET between fluorescent proteins attached to their intracellular domains. We used the fundamental measure of FRET, efficiency (*E*), defined as the proportion of all donor excited states that are transferred to acceptor (Zal and Gascoigne, 2004) to detect an increase in donor proximity to acceptor. We previously demonstrated that the FRET signal between CD3ζ-CFP and CD8β-YFP is specifically induced by antigen recognition and not simply caused by diffusion-driven interactions due to increased crowding of the molecules (Yachi et al., 2005). FRET was not increased by nonstimulatory ligands alone, in synapses with similar amounts of TCR and coreceptor (Yachi et al., 2005; Zal et al., 2002). FRET imaging provides sensitive detection of fine differences in protein interactions in subcellular compartments.

With most APLs, we observed a simple relationship between solution binding kinetics, recruitment of CD3 and induction of CD3ζ-CD8β FRET within the synapse, and the overall bioactivity of the ligand. For example, OVA showed strong and early conjugate formation and recruitment of both CD8 and CD3ζ to the synapse, with induction of a strong FRET signal. OVA is a strong agonist and negative selector and has a relatively high affinity and long half-life for TCR binding. Similarly, the antagonists and positive selectors E1 and R4 have lower affinities and shorter half-lives than OVA (Alam et al., 1996) and induced weak FRET responses. It is perhaps noteworthy that E1 is not only a stronger antagonist than R4, but also a very weak agonist (Hogquist et al., 1994). In agreement, E1 gives an earlier and stronger FRET response than R4. This relatively simple relationship

between TCR-pMHC binding, synapse formation, and CD8β-CD3ζ FRET induction, and the biological outcome of stimulation by the APL, does not hold in all cases. G4 is an interesting intermediate APL in the OT-I system. It can act as agonist and antagonist, giving positive selection in FTOC. However, it stimulates OT-I cells only at high concentration and after long time periods compared to OVA stimulation (Rosette et al., 2001). It has a very long half-life and very slow association rate compared to OVA. Its time course for T-APC conjugate formation, CD3ζ recruitment, and FRET was delayed in comparison to OVA, yet the FRET signal was as strong as that of OVA. These data suggest that the slow induction of CD3ζ-CD8 interaction, and as a result the slow T cell activation, is due to the slow on rate of the TCR binding to K^b-G4. Once made, this interaction is stable, supporting accumulation of interactions between the TCR-CD3 complex and CD8, and therefore increased but delayed FRET response. Overall, this interplay between TCR-pMHC binding and induction of CD8β-CD3ζ interaction can explain the T cell activation phenotype.

A different relationship between biological activity and binding kinetics is shown by A2, which is only 10%–20% as strong an agonist as OVA, but has a similar affinity and longer half-life (Alam et al., 1999). It is also a weaker negative selector. Instead of complete deletion of OT-I thymocytes, it selects cells with CD8αα rather than CD8αβ, which are unable to mount a strong response to OVA (Hogquist et al., 1995). This type of "agonist selection" results in cells that are exiled to patrol the far provinces of the T cell empire, such as the gut and epithelium, to stand in the front line of immune defense together with innate immune cells (Cheroutre, 2004). Induction of CD8β-CD3ζ FRET was weaker and slightly delayed compared to OVA, and recognition of A2 was more sensitive to CD8 Ab blocking. Thus, the timing of TCR-CD8 interaction induced by A2 correlated with its biological properties despite anomalous solution binding kinetics.

Although CD8 binds K^b-A2, the A2 peptide might change K^b conformation so as to alter docking of CD8 or TCR, changing the architecture of the CD8-pMHC-TCR complex and potentially reducing Lck activity. The p2 residue is buried in the structure of K^b. Though not available to the TCR, buried residues can influence the structure of other parts of the peptide or of the surface of the MHC (Fremont et al., 1995). Some OVA p2 variants affect Ab-defined K^b epitopes (Hogquist et al., 1993). Although alanine at p2 does not alter these epitopes (K. Hogquist, personal communication), it is possible that conformational changes caused by A2 are undetectable by the available Abs. In this context, it is of interest that the TCR CDR2α binds K^b near p2. Subtle changes in the binding position of CDR2α on pMHC have been suggested to influence the CD8 dependence of the TCR (Buslepp et al., 2003). Poor CD8 compatibility for the TCR-pMHC complex could explain why the solution binding is stronger than expected for the functionality for this peptide. This supports the idea that the ability to engage CD8 is somewhat peptide dependent and, like TCR-pMHC binding, is important in distinguishing pMHC complexes by TCR (Daniels and Jameson, 2000).

Our data showed a time lag between conjugate formation, TCR recruitment to the synapse, and interaction between CD8β and CD3ζ during recognition of some APLs. This was clearest for functionally weaker APLs, where TCR recruitment and TCR-CD8 interaction were delayed compared to strong agonist. This time lag in TCR-CD8 interaction and the dependence of the type of signal (agonist, antagonist, etc.) on the induction of the TCR-CD8 interaction fits well with a coreceptor kinetic proofreading model of T cell activation (Germain, 2001). This model predicts that certain biochemical events occur at distinct times, so the timing of coreceptor and Lck recruitment to the TCR leads to distinct signaling by the T cell. Therefore, TCR complex phosphorylation at later time points by Lck leads to qualitatively different signaling compared to early phosphorylation, because other biochemical events interfere differently with the signal. This model requires a time delay between the TCR's encounter with pMHC before CD8 can interact with the TCR. We have directly shown that there is a time lag and that it is prolonged for functionally weaker APLs, as predicted by this model from their lower TCR-pMHC affinities. The reduced FRET signal for weaker APLs also agrees with this model, as the likelihood of forming a stable TCR-pMHC interaction able to recruit CD8 reduces with weaker affinities. The importance of timing in initiation of the CD8-TCR interaction can be understood through competing positive and negative feedback loops, such as that described between ERK and SHP-1 (Stefanova et al., 2003). SHP-1 is recruited to the TCR by antagonists, where it inactivates Lck. Agonists activate ERK as well as SHP-1. Phospho-ERK phosphorylates TCR-associated Lck on a serine residue so that it cannot bind to pSHP-1. As ERK activation is downstream of Lck phosphorylation of CD3ζ, CD8-Lck recruitment to the TCR plays an important role in this feedback loop. The longer it takes for CD8-TCR interaction to occur, and therefore for Lck to start signaling leading to ERK activation, the more SHP-1 can be recruited to the TCR complex to inhibit any further signaling.

We propose that the biological property of a given pMHC is not governed solely by TCR binding but rather by the composite ability to engage TCR and the coreceptor and to properly align the coreceptor and TCR in this multimolecular complex. In other words, it is possible that a pMHC ligand may offer a good fit for TCR (as seen by high affinity and/or long half-life), but at the same time may compromise engagement of the coreceptor or the ideal membrane alignment between the TCR and the coreceptor. Such a pMHC ligand would then be a weaker agonist than a ligand that offers an optimal balance between binding of TCR and coreceptor and their alignment in the membrane, even if that involves a lower TCR affinity. This notion may help explain why TCR affinities are so low. The affinities selected during thymic selection ensure that the TCR has to take advantage of coreceptor in order to produce a functional response, at least at low levels of antigen. This mechanism ensures exquisite selectivity of T cell activation by the appropriate class of MHC molecule and provides a fail-safe mechanism to avoid inadvertent T cell activation by random cell-surface proteins or viral products that happen to bind TCR with appropriate affinity. This

view of balanced TCR and coreceptor alignment upon pMHC recognition differs from the prevalent view where coreceptor is simply a passive enhancer of activation and allows reconciliation of conflicting solution TCR-pMHC binding data.

This study highlights the importance of CD8 being a separate molecule from the TCR and its interaction with TCR being inducible by pMHC: minor structural changes in pMHC can cause significant changes in the membrane alignment of the components in a multimolecular complex, changing the likelihood of CD8-TCR interaction and therefore the signaling outcome. Thus, CD8 ensures that the TCR can specifically distinguish between structurally very similar peptides via the kinetics of CD8 recruitment to the TCR to translate the TCR-pMHC interaction into a biological response.

Experimental Procedures

Reagents and Cells

Peptides were synthesized at the TSRI Core Facility and purified by HPLC. The sequence of OVA is SIINFEKL, and APLs are specified by the altered residue and its position in this sequence. Thus, G4 is SIIGFEKL. The sequences of all the peptides used in this study are presented in Table S1. Rabbit polyclonal anti-pERK1 and pERK2 was obtained from Santa Cruz Biotechnology (Santa Cruz, CA), goat anti (a)-rabbit IgG-Alexa680 from Molecular Probes (Eugene, OR), aCD8α (CT-CD8a) from Caltag (Burlingame, CA), and aH-2K^b (AF6-88.5) and aVβ5 (MR9-4) from BDBiosciences (San Diego, CA). Hybridomas expressing the OT-I TCR and CD8α were a gift of E. Palmer (U. of Basel, Switzerland). They were made by retroviral transfection of TCR-deficient 58$\alpha^-\beta^-$ cells with the following genes (with selection marker): OT-I α chain (G418), OT-I β-chain (puromycin), and CD8α (histidinol). Cells expressing the appropriate cell-surface proteins were FACS sorted and cloned (Stotz et al., 1999). The CD8β-YFP (Yachi et al., 2005) and CD3ζ-CFP (Zal et al., 2002) constructs have been described previously. In brief, CD8β and CD3ζ were fused at their C termini with YFP or CFP, respectively, with spacers between the two molecules to allow proper folding and flexibility. These constructs were inserted into pBMN-Z, a retroviral expression vector based on LZRS-LacZ(A) (Kinsella and Nolan, 1996) without EBV sequences (http://www.stanford.edu/group/nolan). Virus was produced from Phoenix packaging cells (gift of G. Nolan) and used to infect OT-I cells as described (Yachi et al., 2005). Cells were maintained in IMDM (OT-I) or RPMI (RMA-S) containing 10% FCS, 2 mM L-glutamine, 100 U/ml penicillin/streptomycin, and 50 μM β-mercaptoethanol. For selection, 500 μg/ml G418 (for TCRα) and 3 μg/ml puromycin (for TCRβ) were used. Because optimal sensitivity of FRET with donor-ratioed sensitized emission or *E* requires that the acceptor is not limiting, we used cells with a donor:acceptor molar ratio of 1:1 to 1:3 calibrated by imaging and comparison with a stoichiometric CFP-YFP construct.

Antigen-Presenting Cell Preparation

RMA-S cells were stained with Cy5 20 hr prior to experiments by incubating cells with 0.1 mg/ml of Cy5 succinimidyl ester (Amersham Biosciences, Bucks, UK) in RPMI at RT for 5 min, washing, and quenching with 10% FCS in RPMI. The RMA-S cells were incubated at 29°C overnight, pulsed with peptides for 30 min at 29°C, incubated at 37°C for 3 hr, and washed once.

TCR Downregulation and Conjugate Formation Assays

1×10^5 OT-I hybridomas and 1×10^5 peptide-pulsed RMA-S cells were added to 96-well round bottom wells in a total volume of 50 μl and incubated for the indicated times at 37°C. After incubation, the cells were stained for Vβ5 and examined by flow cytometry. The data are shown as a percentage of Vβ5 expression on the surface of cells compared to cells incubated with RMA-S without peptide. For the conjugate formation assay, the cells were pipetted up and down three times after the incubation period before fixing in 2% paraformaldehyde at indicated time points. After fixing for 12 min at RT, the cells were washed in PBS and the paraformaldehyde was inactivated by 10 mM Tris (pH 7.4) in PBS for 5 min at RT. The cell conjugates were examined by flow cytometry based on simultaneous expression of YFP (OT-I hybridoma) and Cy5 (Cy5-labeled RMA-S cell).

CTL Assay for CD8 Dependency

OT-I CTLs were derived from stimulation of OT-I spleen cells for 5 days with peptide-pulsed irradiated (2000R) B6 spleen cells. A standard ^{51}Cr-release assay was performed with ^{51}Cr-labeled EL-4 cells. EL-4 cells were loaded with either 20 μM of OVA peptide or 80 μM of A2 for 1 hr. These levels were determined to give equivalent levels of killing in titration experiments. Control targets included EL-4 cells in the absence of peptide, non-^{51}Cr-labeled EL-4 cells, ^{51}Cr-labeled EL-4 cells incubated with a lysis buffer. OT-I CTL were incubated with varying concentrations of CD8α Ab (CT-CD8a) for 30 min on ice before adding the EL-4 cells. Control effector cells were OT-I CTLs without Ab. The assays were performed in 96-well round bottom wells at a 5:1 effector:target ratio (10^5 CTLs with 2×10^4 EL-4 cells/well) in a total volume of 200 μl. The cells were incubated for 4 hr, and 100 μl was removed for counting.

Intracellular Staining for pERK

10^5 OT-I hybridomas and 10^5 peptide-pulsed RMA-S cells were added to 96-well round bottom wells in a total volume of 50 μl and incubated for the indicated times at 37°C. Cells were fixed as described above, washed, and permeabilized with 0.2% saponin in PBS for 10 min at RT, then stained with pERK Ab for 1 hr. Cells were washed twice with PBS-saponin, then stained with anti-rabbit IgG-alexa680 for 45 min in a FACS buffer containing saponin, washed, and mounted in Slowfade Light antifade mounting medium (Molecular Probes) for imaging.

Microscopy

A system specifically designed for FRET microscopy was used, consisting of Slidebook 4.0.3.9 software (3I Corp, Denver, CO) running a Zeiss 200M microscope and two CoolSnapHQ cameras (Roper, Tucson, AZ) attached through a beam-splitter (510LPXR, Chroma), allowing simultaneous acquisition of donor and acceptor emission. Rapid excitation switching was performed with a DG4 galvo illuminator with a 300W xenon lamp (Sutter, Novato, CA). YFP excitation was attenuated to 20% by dynamic positioning of the exit mirror. Optical filters (Chroma) were: a common dichroic mirror JP4, YFPex 510/20 nm, YFPem 550/50 nm, CFPex 430/25 nm, CFPem 470/30 nm, Cy5ex 622/36 nm, Cy5em 700/75 nm. Exposure times were 0.2–0.8 s with 2 × 2 binning and Zeiss 63 × 1.4 Planapo oil objective. Live cells were imaged in HEPES-buffered 199 (low autofluorescence: GIBCO, Grand Island, NY) with 5% FCS, no antibiotics, maintained at 37°C by the FCS2 live imaging chamber and objective heater (Bioptechs, Butler, PA). T cells and peptide-loaded RMA-S cells were briefly mixed and added into a prewarmed imaging chamber coated with poly-D-lysine (Sigma). For fixed cell imaging, the cells were treated as above.

CFP, YFP Imaging, and FRET Analysis

A 3-filter set algorithm for calculation of FRET efficiency (*E*) was used as described (Zal and Gascoigne, 2004; Zal et al., 2002). For each focal position, three exposures were registered: I_{DD} (donor excitation/emission), I_{AA} (acceptor excitation/emission), and I_{DA} (donor excitation/acceptor emission, called CY). Background was subtracted based on a user-specified, cell-free region of each image after software flat-field correction. Images were registered with subpixel accuracy with automated Slidebook software registration function. The bleed-through coefficients of CFP into CY image and YFP into CY image were calibrated with cells expressing either CD3ζ-CFP or CD8β-YFP alone. YFP→CY bleed-through a = 8.8% and CFP→CY bleed-through d = 63%. FRET efficiency was calculated as $E_{app} = (I_{DA} - a^*I_{AA} - dI_{DD})/(I_{DA} - a^*I_{AA} - dI_{DD} + GI_{DD})$ (Zal and Gascoigne, 2004; Zal et al., 2002). G = 3.5 ± 0.1 (Gordon parameter) is the independently calibrated ratio of sensitized emission in the I_{DA} filter set before photobleaching to donor recovery in the I_{DD} filter set after acceptor photobleaching (Gordon et al., 1998; Zal and Gascoigne, 2004). Cells with unusually high or low CD8β-YFP/CD3ζ-CFP ratios (outside the 1:1 to 3:1 stoichiometric range), as well as movement

artifacts, were excluded from analysis. The average FRET was calculated from the contact interface. Statistical differences were calculated by the mean difference hypothesis of Student's two-tailed t test assuming different variances and confidence level of 95%.

Supplemental Data

One Supplemental Table can be found with this article online at http://www.immunity.com/cgi/content/full/25/2/203/DC1/.

Acknowledgments

We thank Ed Palmer (University of Basel) and Garry Nolan (Stanford University) for their generous gifts of reagents. This work was supported by NIH grants R01GM065230 and R01GM039476 to N.R.J.G. and T32AI07290 to T.Z. This is manuscript IMM-16659 from The Scripps Research Institute.

Received: February 27, 2006
Revised: April 21, 2006
Accepted: May 11, 2006
Published online: July 27, 2006

References

Alam, S.M., Travers, P.J., Wung, J.L., Nasholds, W., Redpath, S., Jameson, S.C., and Gascoigne, N.R.J. (1996). T cell receptor affinity and thymocyte positive selection. Nature *381*, 616–620.

Alam, S.M., Davies, G.M., Lin, C.M., Zal, T., Nasholds, W., Jameson, S.C., Hogquist, K.A., Gascoigne, N.R.J., and Travers, P.J. (1999). Qualitative and quantitative differences in T cell receptor binding of agonist and antagonist ligands. Immunity *10*, 227–237.

Buslepp, J., Wang, H., Biddison, W.E., Appella, E., and Collins, E.J. (2003). A correlation between TCR Va docking on MHC and CD8 dependence: implications for T cell selection. Immunity *19*, 595–606.

Cheroutre, H. (2004). Starting at the beginning: new perspectives on the biology of mucosal T cells. Annu. Rev. Immunol. *22*, 217–246.

Chidgey, A.P., and Boyd, R.L. (1998). Positive selection of low responsive, potentially autoreactive T cells induced by high avidity, non-deleting interactions. Int. Immunol. *10*, 999–1008.

Daniels, M.A., and Jameson, S.C. (2000). Critical role for CD8 in T cell receptor binding and activation by peptide/major histocompatibility complex multimers. J. Exp. Med. *191*, 335–346.

Fremont, D.H., Stura, E.A., Matsumura, M., Peterson, P.A., and Wilson, I.A. (1995). Crystal structure of an H-2K^{b}-ovalbumin peptide complex reveals the interplay of primary and secondary anchor positions in the major histocompatibility complex binding groove. Proc. Natl. Acad. Sci. USA *92*, 2479–2483.

Gao, G.F., Tormo, J., Gerth, U.C., Wyer, J.R., McMichael, A.J., Stuart, D.I., Bell, J.I., Jones, E.Y., and Jakobsen, B.K. (1997). Crystal structure of the human CD8aa and HLA-A2. Nature *387*, 630–634.

Gascoigne, N.R.J., and Zal, T. (2004). Molecular interactions at the T cell-antigen-presenting cell interface. Curr. Opin. Immunol. *16*, 114–119.

Gascoigne, N.R.J., Zal, T., and Alam, S.M. (2001). T-cell receptor binding kinetics in T-cell development and activation. Expert Rev. Mol. Med. *12 Feb; 2001*, 1–17.

Germain, R.N. (2001). The T cell receptor for antigen: signaling and ligand discrimination. J. Biol. Chem. *276*, 35223–35226.

Gil, D., Schamel, W.W.A., Montoya, M., Sanchez-Madrid, F., and Alarcon, B. (2002). Recruitment of Nck by CD3e reveals a ligand-induced conformational change essential for T cell receptor signaling and synapse formation. Cell *109*, 901–912.

Gordon, G.W., Berry, G., Liang, X.H., Levine, B., and Herman, B. (1998). Quantitative fluorescence resonance energy transfer measurements using fluorescence microscopy. Biophys. J. *74*, 2702–2713.

Hogquist, K.A., Grandea, A.G., 3rd, and Bevan, M.J. (1993). Peptide variants reveal how antibodies recognize major histocompatibility complex class I. Eur. J. Immunol. *23*, 3028–3036.

Hogquist, K.A., Jameson, S.C., Heath, W.R., Howard, J.L., Bevan, M.J., and Carbone, F.R. (1994). T cell receptor antagonist peptides induce positive selection. Cell *76*, 17–27.

Hogquist, K.A., Jameson, S.C., and Bevan, M.J. (1995). Strong agonist ligands for the T cell receptor do not mediate positive selection of functional CD8^{+} T cells. Immunity *3*, 79–86.

Holmberg, K., Mariathasan, S., Ohteki, T., Ohashi, P.S., and Gascoigne, N.R.J. (2003). TCR binding kinetics measured with MHC class I tetramers reveal a positive selecting peptide with relatively high affinity for TCR. J. Immunol. *171*, 2427–2434.

Jameson, S.C., Hogquist, K.A., and Bevan, M.J. (1994). Specificity and flexibility in thymic selection. Nature *369*, 750–752.

Kinsella, T.M., and Nolan, G.P. (1996). Episomal vectors rapidly and stably produce high-titer recombinant retrovirus. Hum. Gene Ther. *7*, 1405–1413.

Kjer-Nielsen, L., Clements, C.S., Purcell, A.W., Brooks, A.G., Whisstock, J.C., Burrows, S.R., McCluskey, J., and Rossjohn, J. (2003). A structural basis for the selection of dominant ab T cell receptors in antiviral immunity. Immunity *18*, 53–64.

Ljunggren, H.G., Stam, N.J., Ohlen, C., Neefjes, J.J., Hoglund, P., Heemels, M.T., Bastin, J., Schumacher, T.N., Townsend, A., Karre, K., and Ploegh, H. (1990). Empty MHC class I molecules come out in the cold. Nature *346*, 476–480.

Madrenas, J., Chau, L.A., Smith, J., Bluestone, J.A., and Germain, R.N. (1997). The efficiency of CD4 recruitment to ligand-engaged TCR controls the agonist/partial agonist properties of peptide-MHC molecule ligands. J. Exp. Med. *185*, 219–229.

Norment, A.M., Salter, R.D., Parham, P., Engelhard, V.H., and Littman, D.R. (1988). Cell-cell adhesion mediated by CD8 and MHC class I molecules. Nature *336*, 79–81.

Risueno, R.M., van Santen, H.M., and Alarcon, B. (2006). A conformational change senses the strength of T cell receptor-ligand interaction during thymic selection. Proc. Natl. Acad. Sci. USA *103*, 9625–9630.

Rosette, C., Werlen, G., Daniels, M.A., Holman, P.O., Alam, S.M., Travers, P.J., Gascoigne, N.R.J., Palmer, E., and Jameson, S.C. (2001). The impact of duration versus extent of TCR occupancy on T cell activation: a revision of the kinetic proofreading model. Immunity *15*, 59–70.

Sebzda, E., Kündig, T.M., Thomson, C.T., Aoki, K., Mak, S.Y., Mayer, J.P., Zamborelli, T., Nathenson, S.G., and Ohashi, P.S. (1996). Mature T cell reactivity altered by peptide agonist that induces positive selection. J. Exp. Med. *183*, 1093–1104.

Starr, T.K., Jameson, S.C., and Hogquist, K.A. (2003). Positive and negative selection of T cells. Annu. Rev. Immunol. *21*, 139–176.

Stefanova, I., Hemmer, B., Vergelli, M., Martin, R., Biddison, W.E., and Germain, R.N. (2003). TCR ligand discrimination is enforced by competing ERK positive and SHP-1 negative feedback pathways. Nat. Immunol. *4*, 248–254.

Stotz, S.H., Bolliger, L., Carbone, F.R., and Palmer, E. (1999). T cell receptor (TCR) antagonism without a negative signal: evidence from T cell hybridomas expressing two independent TCRs. J. Exp. Med. *189*, 253–263.

Veillette, A., Bookman, M.A., Horak, E.M., and Bolen, J.B. (1988). The CD4 and CD8 T cell surface antigens are associated with the internal membrane tyrosine-protein kinase p56lck. Cell *55*, 301–308.

Werlen, G., Hausmann, B., Naeher, D., and Palmer, E. (2003). Signaling life and death in the thymus: timing is everything. Science *299*, 1859–1863.

Yachi, P.P., Ampudia, J., Gascoigne, N.R.J., and Zal, T. (2005). Nonstimulatory peptides contribute to antigen-induced CD8-T cell receptor interaction at the immunological synapse. Nat. Immunol. *6*, 785–792.

Zal, T., and Gascoigne, N.R.J. (2004). Photobleaching-corrected FRET efficiency imaging of live cells. Biophys. J. *86*, 3923–3939.

Zal, T., Zal, M.A., and Gascoigne, N.R.J. (2002). Inhibition of T-cell receptor-coreceptor interactions by antagonist ligands visualized by live FRET imaging of the T-hybridoma immunological synapse. Immunity *16*, 521–534.